



Article

# Conformational Restriction of Histamine with a Rigid Bicyclo[3.1.0]hexane Scaffold Provided Selective H<sub>3</sub> Receptor Ligands

Mizuki Watanabe <sup>1,\*</sup> , Takaaki Kobayashi <sup>1</sup>, Yoshihiko Ito <sup>2</sup>, Shizuo Yamada <sup>2</sup> and Satoshi Shuto <sup>1,3,\*</sup> 

<sup>1</sup> Faculty of Pharmaceutical Sciences, Hokkaido University, Kita-12, Nishi-6, Kita-ku, Sapporo 060–0812, Japan; kobayashit27@sc.sumitomo-chem.co.jp

<sup>2</sup> Center for Pharma-Food Research (CPFR), Graduate School of Pharmaceutical Sciences, University of Shizuoka, 52-1, Yada, Suruga-ku, Shizuoka 422–8526, Japan; y-ito@u-shizuoka-ken.ac.jp (Y.I.); yamada@u-shizuoka-ken.ac.jp (S.Y.)

<sup>3</sup> Center for Research and Education on Drug Discovery, Hokkaido University, Kita-12, Nishi-6, Kita-ku, Sapporo 060–0812, Japan

\* Correspondence: mwatanab@pharm.hokudai.ac.jp (M.W.); shu@pharm.hokudai.ac.jp (S.S.)

Academic Editor: Marie Migaud

Received: 16 July 2020; Accepted: 4 August 2020; Published: 5 August 2020



**Abstract:** We designed and synthesized conformationally rigid histamine analogues with a bicyclo[3.1.0]hexane scaffold. All the compounds were selectively bound to the H<sub>3</sub> receptor subtype over the H<sub>4</sub> receptor subtype. Notably, compound 7 showed potent binding affinity and over 100-fold selectivity for the H<sub>3</sub> receptors ( $K_i = 5.6$  nM for H<sub>3</sub> and 602 nM for H<sub>4</sub>). These results suggest that the conformationally rigid bicyclo[3.1.0]hexane structure can be a useful scaffold for developing potent ligands selective for the target biomolecules.

**Keywords:** histamine; H<sub>3</sub> receptor; conformational restriction; selective ligands

## 1. Introduction

Histamine (**1**, Figure 1), a monoamine chemical mediator, acts on four different receptor subtypes, H<sub>1</sub>, H<sub>2</sub>, H<sub>3</sub>, and H<sub>4</sub> receptors, which are members of the G protein-coupled receptor superfamily. In early the 1980s, the histamine H<sub>3</sub> receptor (H<sub>3</sub>R) was identified as a presynaptic autoreceptor in rats [1], and the human H<sub>3</sub>R was cloned in 1999 [2]. The H<sub>3</sub>R, which is mainly expressed in the central nervous system (CNS), not only acts as an autoreceptor to regulate the central levels of histamine but also acts as a heteroreceptor to regulate the synthesis and release of other neurotransmitters, such as noradrenaline, acetylcholine, dopamine, and serotonin, and it is involved in various physiological processes, including memory function, cognition, anxiety, pain, food intake, and body temperature regulation. Thus, H<sub>3</sub>R activity inhibition could be a potential treatment for various CNS-related disorders, such as attention-deficit hyperactivity disorder, Alzheimer’s disease, narcolepsy, Parkinson’s disease, schizophrenia, and obesity. Much effort has been devoted to developing potent and selective H<sub>3</sub>R inhibitors (antagonists/inverse agonists) [3–5], and pitolisant (**2**, Figure 1) was recently authorized in Europe as a medicine for treating narcolepsy with or without cataplexy [6]. Further research is needed to better understand the functions of the histaminergic system in CNS-related disorders and to advance useful H<sub>3</sub> antagonists into clinical trials and the market [7].

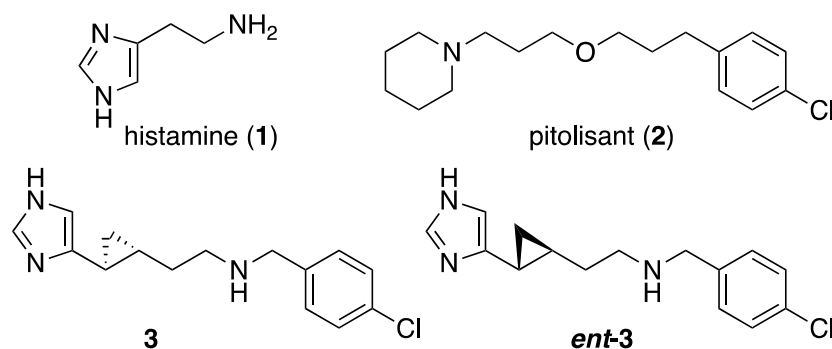


**Figure 1.** Chemical structures of histamine (1), pitolisant (2), and cyclopropane-based conformationally restricted histamine analogues as H<sub>3</sub>/H<sub>4</sub> antagonists (3 and *ent*-3).

The development of efficient H<sub>3</sub>-selective antagonists is often complicated by the high affinity of H<sub>3</sub> antagonists for the H<sub>4</sub> receptor (H<sub>4</sub>R) because the structures of the two receptor subtypes are presumed to be analogous due to their highly homologous gene sequences (58% identity in the transmembrane regions) [8,9]. However, precise three-dimensional structural information of H<sub>3</sub>R and H<sub>4</sub>R is unavailable, because their X-ray crystal structures have not been reported. To efficiently develop bioactive ligands, even if the structural information of the target proteins is unknown, we developed a three-dimensional structural diversity-oriented strategy based on the characteristic structural properties of chiral cyclopropane, which is the rigid and smallest carbocyclic structure [10]. Introducing cyclopropane into the conformationally flexible acyclic backbone of a parent compound can restrict the conformation of the molecule in either its *trans*- or *cis*-form. That is, four stereoisomer derivatives, including the enantiomers, can be produced from one parent ligand, in which the functional groups essential for the binding to a target protein can be restricted in different spatial arrangements. Therefore, one restricted structure of these isomers may be analogous to the bioactive form of the parent ligand, resulting in the discovery of a lead compound that is superior to the prototype ligand in its target selectivity and/or binding potency [11–15]. Based on this strategy, we previously designed and synthesized a series of cyclopropane-based conformationally restricted histamine analogues having an imidazolylcyclopropane scaffold and identified **3** and its enantiomer *ent*-**3** as potent H<sub>3</sub> antagonists ( $K_i$ : 3.6 nM and 8.4 nM for the H<sub>3</sub>R, respectively, shown in Figure 1) [16]. These antagonists have high binding affinities for the H<sub>3</sub>R; however, the selectivity between H<sub>3</sub>R and H<sub>4</sub>R is insufficient with selectivity ratios for H<sub>4</sub>/H<sub>3</sub> of 10.3 (**3**) and 0.9 (*ent*-**3**). Thus, in this study, to obtain more highly selective ligands for H<sub>3</sub>R, we adopted bicyclo[3.1.0]hexane as a more rigid scaffold for newly designed conformationally restricted histamine analogues [17].

## 2. Results

### 2.1. Design

We assumed that the reason for the low H<sub>4</sub>/H<sub>3</sub> selectivity of **3** and *ent*-**3** was the flexibility of the aminoalkyl side chain in the compounds. Although the backbone conformation is restricted to the *trans*-configuration, there are two conformers, *anti*- and *syn*-form, whose aminoalkyl chains orient to the side opposite and same to the cyclopropane ring, respectively, due to the C2–C3 bond rotation (Figure 2a). This bond rotation is limited by the “cyclopropylic strain” that causes a sizable steric repulsion similar to the 1,3-allylic strain between the two adjacent *cis*-configured substituents, which are fixed in an eclipse orientation on the cyclopropane ring. The stable conformation is where the smallest group on the C3 position orients inward to the cyclopropane ring. Conformational analysis using MacroModel 8.6 showed that the *anti*- and *syn*-forms of **3** are the two most stable conformations ( $\Delta E = 0.3$  kcal/mol), whereas the A-form of **3** is extremely unstable due to the cyclopropylic strain ( $\Delta E > 3$  kcal/mol, relative potential energy from the global minimum; Figure 2a).

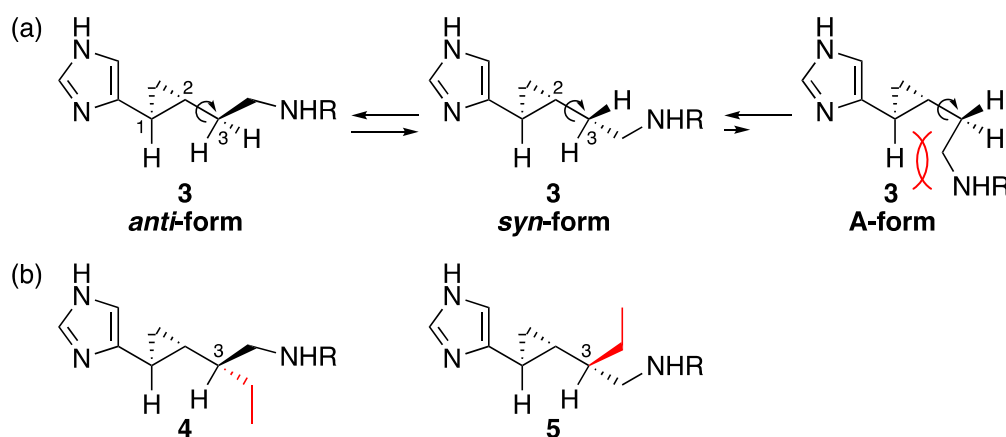


**Figure 2.** (a) The *anti*-, *syn*- and A-forms in 3; (b) The conformationally restricted histamine analogues 4 and 5 with cyclopropyl strain. R indicates a 4-chlorobenzyl group.

We designed and synthesized the C3-ethyl-substituted derivatives 4 and 5, as side-chain conformation-restricted analogues of 3 (Figure 2b) [18]. Introducing an ethyl group into the C3 position of 3 prevents the rotation of the side aminoalkyl-chain moiety to effectively restrict the conformation due to the cyclopropyl strain [10]. Accordingly, depending on the configuration at the C3 position, the conformation of the compounds can be restricted to the *anti*-form in 4 and the *syn*-form in 5. The biological evaluation for H<sub>3</sub>R demonstrated that the *anti*-restricted 4 exhibited high binding affinity for H<sub>3</sub>R ( $K_i = 6.7$  nM) comparable to 3; on the other hand, the binding affinity of *syn*-restricted 5 for H<sub>3</sub>R ( $K_i = 63.0$  nM) was more than 15-fold lower than that of 3. These results showed that the conformational restriction of the side chain to the *anti*- or *syn*-form affects the binding affinity to the target protein. Unfortunately, however, further biological assay showed that 4 and 5 not only bound to H<sub>3</sub>R but also to H<sub>4</sub>R and were non-selective for the two receptor subtypes (selectivity ratios for H<sub>4</sub>/H<sub>3</sub> of 1.2–1.3, Table 1).

**Table 1.** Binding affinities of the compounds for the human H<sub>3</sub> and H<sub>4</sub> receptor subtypes.<sup>a</sup>

Compound	Form	H <sub>3</sub> , K <sub>i</sub> (nM)	H <sub>4</sub> , K <sub>i</sub> (nM)	Selectivity Ratio (H <sub>4</sub> /H <sub>3</sub> )
6	<i>anti</i>	31.6 ± 8.2	501 ± 201	16
7	<i>syn</i>	5.6 ± 1.6	602 ± 343	108
<i>ent</i> -6	<i>anti</i>	21.9 ± 6.0	416 ± 155	19
<i>ent</i> -7	<i>syn</i>	14.8 ± 3.8	69.2 ± 21	4.7
3 <sup>b</sup>	–	3.6 ± 0.4	37.2 ± 2.7	10
<i>ent</i> -3 <sup>b</sup>	–	8.4 ± 1.5	7.6 ± 0.4	0.9
4	<i>anti</i>	6.7 ± 0.4 <sup>c</sup>	9.0 ± 1.0	1.3
5	<i>syn</i>	63.0 ± 6.1 <sup>c</sup>	76.5 ± 14	1.2
Thioperamide <sup>b</sup>	–	51 ± 3.8	124 ± 14	2.4

<sup>a</sup> Data are expressed as means ± SEM (n = 3–5). <sup>b,c</sup> Data were taken from [16] (b) and [18] (c).

Taking these results into account, we planned to obtain highly selective ligands for H<sub>3</sub>R by adopting an alternative strategy that utilizes a rigid fused-ring structure as a scaffold (Figure 3). Cyclopropane-based conformationally restricted ligands have two side-chain orientations, *anti* and *syn*, as described above. The introduction of a "branch" substituent on the cyclopropane adjacent carbon in the side-chain allows the orientation to be restricted to *anti* or *syn* due to the cyclopropyl strain, depending on the configuration at the cyclopropane adjacent carbon. On the other hand, instead of utilizing the cyclopropyl strain, the side-chain orientation can be restricted to *anti* or *syn* by introducing a "splint" structure between the cyclopropane and the side chain to form a rigid bicyclo structure. Both of these different conformational restriction strategies can generate the *anti*- and *syn*-restricted cyclopropane derivatives. However, even if they are the same *anti*- or *syn*-restricted

analogues, the difference in the branch and splint units introduced to regulate the conformation may cause different biological profiles. Therefore, in this study, we newly designed conformationally restricted histamine analogues **6**, **7**, and their enantiomers *ent-6*, *ent-7* with a bicyclo[3.1.0]hexane scaffold that can restrict the spatial arrangement of the imidazole and the aminoalkyl chain (Figure 4). The aminoalkyl chains of **6** and **7** were restricted to *anti* or *syn*, respectively, because the splint “two-carbon unit” forming the bicyclo backbone can lock the C2–C3 bond rotation. We previously used the bicyclo[3.1.0]hexane structure as a backbone for conformationally restricted analogues of  $\gamma$ -aminobutyric acid (GABA) and reported the first potent and selective inhibitor of BGT-1, which is a GABA transporter subtype [19]. Thus, we expected that the conformationally restricted histamine analogues with the bicyclo[3.1.0]hexane scaffold would show selectivity for H<sub>3</sub>R, in contrast to the previous cyclopropyl strain-based conformationally restricted analogues.

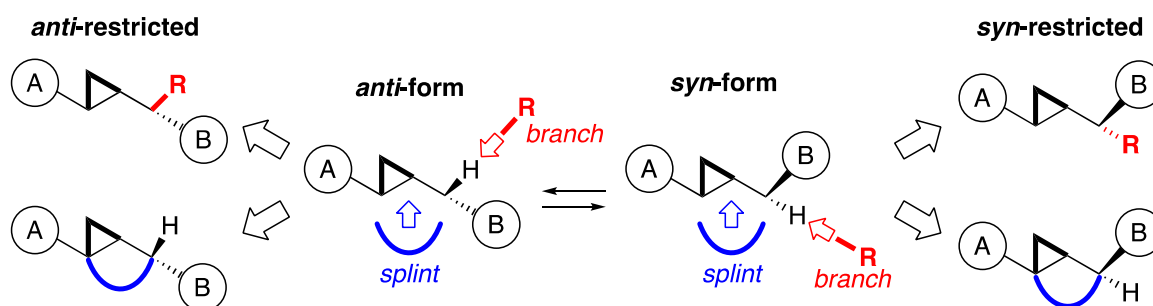


**Figure 3.** The two strategies to conformationally restrict the cyclopropane-based analogues to the *anti*- or *syn*-form by the introduction of a “branch” substituent inducing the cyclopropyl strain or a “splint” moiety forming the bicyclo structure.

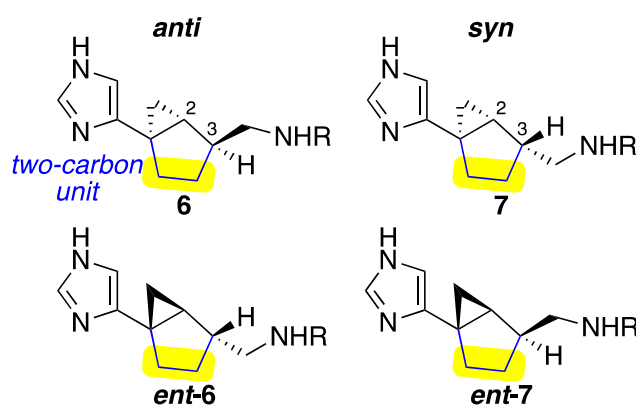
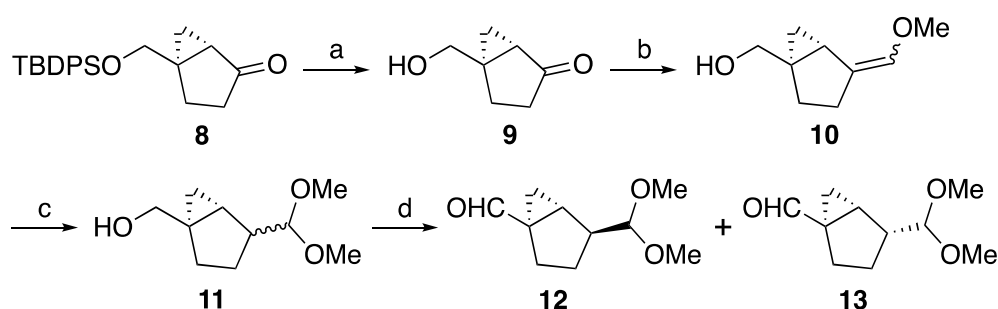


**Figure 4.** The conformationally restricted histamine analogues **6** and **7** with a bicyclo[3.1.0]hexane backbone, and their enantiomers *ent-6* and *ent-7*. R indicates a 4-chlorobenzyl group.

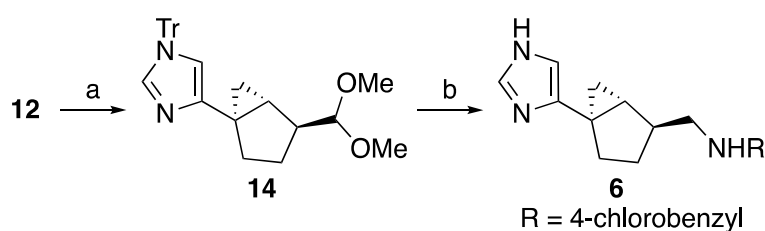
## 2.2. Chemistry

The diastereomerically pure bicyclo[3.1.0]hexane **12** and **13** with all of the asymmetric centers in target compounds **6** and **7**, respectively, were synthesized from ketone **8** [19], which was prepared from (*S*)-epichlorohydrin, as shown in Scheme 1. After removing the *O*-silyl protecting group of **8**, one-carbon addition to **9** was conducted by Wittig reaction to give olefin **10** as an *E/Z* mixture. The treatment of **10** with *p*-toluenesulfonic acid in MeOH under reflux conditions afforded dimethyl acetal **11** as a diastereomeric mixture. Oxidation of the hydroxyl group of **11** and final separation by silica gel column chromatography gave the aldehyde isomers **12** and **13**, respectively.



**Scheme 1.** Reagents and conditions. (a)  $3\text{HF}\cdot\text{Et}_3\text{N}$ , THF, 90%; (b)  $\text{MeOCH}_2\text{PPh}_3\text{Cl}$ ,  $t\text{BuOK}$ , THF,  $0\text{ }^\circ\text{C}$ , 90%; (c)  $\text{TsOH}\cdot\text{H}_2\text{O}$ , MeOH, reflux, 85%; (d)  $\text{SO}_3\cdot\text{pyridine}$ ,  $\text{Et}_3\text{N}$ , DMSO, 29% (**12**) and 52% (**13**).

The conformationally restricted histamine analogue **6** was synthesized from **12** (Scheme 2). The imidazole ring was constructed by treating **12** with tosylmethyl isocyanide, followed by saturated ethanolic ammonia [20]. The resulting unpurified imidazole product was further treated with trityl chloride to afford *N*-tritylimidazolylcyclopropane **14** in 69% overall yield. Removal of the dimethyl acetal group under acidic conditions followed by reductive amination with 4-chlorobenzyl amine gave the desired secondary amine, which was protected by a Boc group for easy purification. Finally, acidic treatment of the protected amine simultaneously removed the *N*-Boc and *N*-Tr groups to provide the desired compound **6**. The diastereomer **7** was similarly prepared from **13** (Scheme S1). Configurations of the C3 position in **6** and **7** were determined based on the nuclear Overhauser effect (NOE) difference spectra (Figure S1). In addition, enantiomers *ent*-**6** and *ent*-**7** were synthesized by the same procedure from *ent*-**8**, which was prepared from (*R*)-epichlorohydrin (Scheme S2).



**Scheme 2.** Reagents and conditions. (a) (1)  $\text{TsCH}_2\text{NC}$ ,  $\text{NaOEt}$ , EtOH,  $0\text{ }^\circ\text{C}$ ; (2) sat.  $\text{NH}_3/\text{EtOH}$ ,  $125\text{ }^\circ\text{C}$ , sealed tube; (3)  $\text{TrCl}$ ,  $\text{Et}_3\text{N}$ ,  $\text{CH}_2\text{Cl}_2$ , 69% in 3 steps; (b) (1)  $\text{HCO}_2\text{H}$ , hexane (2) 4-chlorobenzyl amine,  $\text{NaBH}(\text{OAc})_3$ ,  $\text{MS4}\text{\AA}$ ,  $\text{CH}_2\text{Cl}_2$ ; (3)  $\text{Boc}_2\text{O}$ ,  $\text{Et}_3\text{N}$ , DMAP, MeOH; (4) aq.  $\text{HCl}$ , EtOH, reflux, 49% in 4 steps.

### 2.3. Biological Evaluation

The binding affinities of **6**, **7**, *ent*-**6**, and *ent*-**7** for the human  $\text{H}_3\text{R}$  subtype with [ $^3\text{H}$ ] $N^\alpha$ -methylhistamine and the human  $\text{H}_4\text{R}$  subtype with [ $^3\text{H}$ ]histamine were evaluated using cell membranes expressing human  $\text{H}_3\text{R}$  or  $\text{H}_4\text{R}$  according to the previously reported method, and the results are summarized in Table 1. These conformationally locked compounds, **6**, **7**, *ent*-**6**, and *ent*-**7** had potent binding affinities for  $\text{H}_3\text{R}$ , although their  $K_i$  values were slightly larger than those of their parent compounds **3** or *ent*-**3** [ $K_i$ : **6** (31.6 nM), **7** (5.6 nM) versus **3** (3.6 nM) and *ent*-**6** (21.9 nM), *ent*-**7** (14.8 nM) versus *ent*-**3** (8.4 nM)]. On the other hand, their  $K_i$  values for  $\text{H}_4\text{R}$  were much larger than those of the parents [ $K_i$ : **6** (501 nM), **7** (602 nM) versus **3** (37.2 nM) and *ent*-**6** (416 nM), *ent*-**7** (69.2 nM) versus *ent*-**3** (7.6 nM)]. Thus, compared to the parents, the bicyclo compounds exhibited clearly improved selectivity for  $\text{H}_3\text{R}$ . Notably, **7** showed highly potent binding affinity and more than 100-fold selectivity for  $\text{H}_3\text{R}$  over the  $\text{H}_4\text{R}$ .

### 3. Discussion

Comparison of the most stable conformations of **7** and the *syn*-form in **3** that were obtained by the MacroModel calculations revealed that the imidazole and amino moieties, which are essential for binding to the receptors, are superimposable; however, the splint “two-carbon unit” introduced for forming the bicyclo backbone of **7** is rather bulky and protrudes from the backbone of **3** (Figure 5). Therefore, the higher H<sub>3</sub>R selectivity of the bicyclo compounds than that of the parents (Table 1) suggest that the splint unit in **6** and **7** caused a steric repulsion in the binding mode for H<sub>4</sub>R, resulting in their low affinity for H<sub>4</sub>R. In other words, there seems to be a difference in the three-dimensional structures between H<sub>3</sub>R and H<sub>4</sub>R around the imidazole binding area in their orthosteric sites.

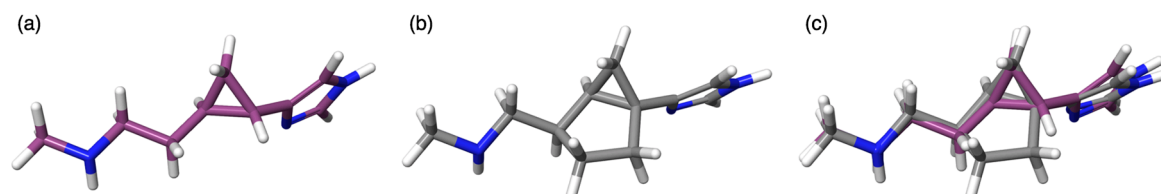


**Figure 5.** The most stable conformation of the *syn*-form in **3** (a) and **7** (b) by conformational search using MacroModel 10.9. (force field: MMFFs, solvent: H<sub>2</sub>O); (c) Superimposition of the stable conformation of **3** and **7**. The chlorobenzyl moiety was replaced with a methyl group to simplify the structures.

The *syn*-restricted **7** with the bicyclo scaffold displayed high selectivity for H<sub>3</sub>R, although the similarly *syn*-restricted **5** with a branched ethyl group for the cyclopropylic strain was non-selective for H<sub>3</sub>R and H<sub>4</sub>R (Table 1). Compared with their three-dimensional structures, the most stable conformations of **5** and **7** calculated by MacroModel are superimposable at the essential imidazole and amino functions (Figure 6). However, the “branch” and “splint” substituents, i.e., the ethyl group introduced to restrict the conformation by the cyclopropylic strain in **5** and the “two-carbon unit” moiety to form the bicyclo scaffold in **7**, are positioned differently in space. In addition, in the most stable conformations of *anti*-restricted **4** and **6**, the imidazole and amino functions are superimposable, but the branch and splint moieties are differently positioned (Figure S3). These results indicate that even when restricted to the same *anti*- or *syn*-form, the “branch” or “splint” moieties that were introduced to restrict the conformation may interact with the target receptor or undergo steric repulsion due to the difference in the spatial arrangement of the moieties, potentially causing the different subtype selectivity. For example, among these four compounds, **4–7**, only **4** had a high binding affinity for H<sub>4</sub>R ( $K_i = 9.0$  nM, Table 1).

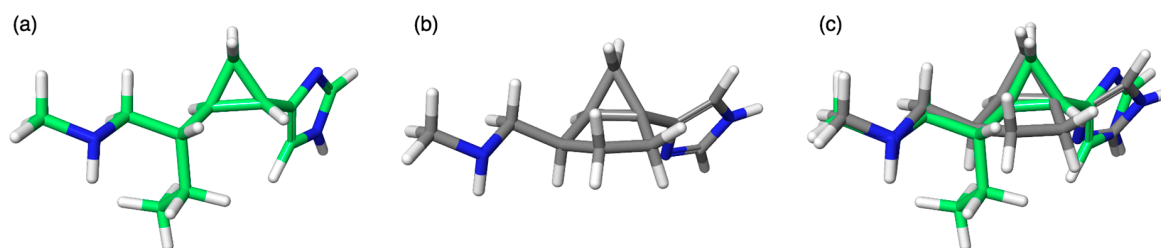


**Figure 6.** The most stable conformation of **5** (a) and **7** (b) by conformational search using MacroModel 10.9. (force field: MMFFs, solvent: H<sub>2</sub>O); (c) Superimposition of the stable conformation of **5** and **7**. The chlorobenzyl moiety was replaced with a methyl group to simplify the structures.

The rigid bicyclo[3.1.0]hexane scaffold was effectively used for the conformational restriction of cyclopropane side chains to improve the H<sub>3</sub>R/H<sub>4</sub>R-selectivity, similar to the previous results in the development of a selective inhibitor for the GABA transporter BGT-1 subtype [19]. On the other hand, the cyclopropylic strain-based conformational restriction strategy has successfully provided a variety of compounds of biological interest, such as NMDA receptor antagonists [21], proteasome

inhibitors [22], melanocortin receptor antagonists [23], and membrane-permeable cyclic peptides [24]. Thus, the two conformational restriction methods using cyclopropane as the key structure effectively complement each other in medicinal chemistry studies for developing potent and selective ligands for various target proteins.

## 4. Materials and Methods

### 4.1. Synthesis

All  $^1\text{H-NMR}$  and  $^{13}\text{C-NMR}$  spectra were recorded on a JEOL JNM-AL-400, JEOL JMM-ECX-400P, or JEOL JMM-ECA-500 spectrometer.  $^1\text{H-NMR}$  chemical shifts are reported as  $\delta$  values in ppm relative to tetramethylsilane (0.00 ppm) when  $\text{CDCl}_3$  was used as the solvent, or a solvent residual peak ( $\text{CD}_2\text{H-OD}$ : 3.31 ppm) when  $\text{CD}_3\text{OD}$  was used as the solvent. Coupling constants ( $J$ ) are reported in Hz, and multiplicity is indicated as follows: s (singlet), d (doublet), dd (double doublet), t (triplet), q (quartet), brs (broad singlet).  $^{13}\text{C-NMR}$  chemical shifts are reported as  $\delta$  values in ppm relative to deuterated solvent ( $\text{CDCl}_3$ : 77.0 ppm or  $\text{CD}_3\text{OD}$ : 49.0 ppm). All mass spectra were obtained on a JEOL JMS-T100LC spectrometer. Elemental analysis was performed with a Yanaco CHN Corder MT-6 or J-Science MICRO CODER JM10 analyzer. Optical rotations were measured with a JASCO P-1030 digital polarimeter. All non-aqueous reactions were carried out under argon atmosphere in anhydrous grade solvents. Silica gel column chromatography was performed using Merck Silica Gel 60, Kanto Silica Gel 60N, or Chromatorex<sup>®</sup> NH-DM1020 (Fuji Silysia Cheical Ltd.). TLC was performed using glass-backed silica gel 60F254.

(1*S*,5*S*)-1-Hydroxymethyl-bicyclo[3.1.0]hexan-4-one (**9**). The mixture of **8** (983 mg, 2.70 mmol) and  $3\text{HF}\cdot\text{Et}_3\text{N}$  (2.2 mL, 6.99 mmol) in THF (25 mL) was stirred at room temperature (rt) for 3 days. The solvent was evaporated, and the residue was purified by flash silica gel column chromatography (hexane/AcOEt, 1/1–0/1) to give **9** (307 mg, 2.43 mmol, 90%) as a colorless liquid.  $[\alpha]_{\text{D}}^{22} = +4.1^\circ$  ( $c$  0.90,  $\text{CHCl}_3$ );  $^1\text{H-NMR}$  (400 MHz,  $\text{CDCl}_3$ )  $\delta$  3.82 (1 H, d,  $J = 11.6$  Hz,  $-\text{CHaHbOH}$ ), 3.66 (1 H, d,  $J = 11.6$  Hz,  $-\text{CHaHbOH}$ ), 2.22–2.09 (4 H, m, H-2, H-3), 1.78 (1 H, dd,  $J = 9.1, 3.2$  Hz, H-5), 1.33 (1 H, dd,  $J = 9.1, 5.0$  Hz, H-6a), 1.19 (1 H, dd,  $J = 5.0, 3.2$  Hz, H-6b);  $^{13}\text{C NMR}$  (100 MHz,  $\text{CDCl}_3$ )  $\delta$  214.98, 64.67, 35.92, 33.00, 31.99, 23.83, 17.55; HRMS (ESI) calcd for  $\text{C}_7\text{H}_{10}\text{NaO}_2$  149.0573, found 149.0573  $[(\text{M} + \text{Na})^+]$ .

(1*S*,5*S*)-1-Hydroxymethyl-4-methoxymethylbicyclo[3.1.0]hexane (**10**, *E/Z*-mixture). To a suspension of methoxymethyltriphenylphosphonium chloride (2.96 g, 8.52 mmol) in THF (20 mL) was added *t*BuOK (ca. 1.0 M solution in THF, 8.0 mL, 8.0 mmol) at 0 °C, and the mixture was stirred at the same temperature for 1 h. To the reaction mixture was added a solution of **9** (307 mg, 2.43 mmol) in THF (4 mL) at 0 °C, and the resulting mixture was stirred at the same temperature for 4 h. After the addition of sat. aq.  $\text{NH}_4\text{Cl}$ , the reaction mixture was concentrated in reduced pressure, and the residue was partitioned between AcOEt and sat. aq.  $\text{NH}_4\text{Cl}$ . The organic layer was washed with brine, dried ( $\text{Na}_2\text{SO}_4$ ), and evaporated. The residue was purified by silica gel column chromatography (hexane/AcOEt, 50/1) to give **10** (338 mg, 2.19 mmol, 90%, *E/Z*-mixture, 1/0.8) as a pale yellow oil.  $[\alpha]_{\text{D}}^{21} = +49.6^\circ$  ( $c$  1.00,  $\text{CHCl}_3$ ); HRMS (ESI) calcd for  $\text{C}_9\text{H}_{14}\text{NaO}_2$  177.0886, found 177.0887  $[(\text{M} + \text{Na})^+]$ ; Major isomer,  $^1\text{H-NMR}$  (400 MHz,  $\text{CDCl}_3$ )  $\delta$  5.85 (1 H, s,  $\text{MeOCH}=\text{C}-$ ), 3.62 (2 H, s,  $-\text{CH}_2\text{OH}$ ), 3.55 (3 H, s,  $\text{CH}_3\text{O}-$ ), 3.02 (1 H, brs, OH), 2.12 (1 H, m, H-3a), 1.97 (1 H, dd,  $J = 8.1, 3.6$  Hz, H-5), 1.93–1.78 (3 H, m, H-2, H-3b), 0.81 (1 H, dd,  $J = 8.1, 4.5$  Hz, H-6a), 0.74 (1 H, m, H-6b);  $^{13}\text{C NMR}$  (100 MHz,  $\text{CDCl}_3$ )  $\delta$  137.57, 121.41, 67.07, 59.14, 33.11, 28.16, 24.60, 22.69, 14.27; Minor isomer,  $^1\text{H-NMR}$  (400 MHz,  $\text{CDCl}_3$ )  $\delta$  5.92 (1 H, s,  $\text{MeOCH}=\text{C}-$ ), 3.62 (2 H, s,  $-\text{CH}_2\text{OH}$ ), 3.53 (3 H, s,  $\text{CH}_3\text{O}-$ ), 3.02 (1 H, brs, OH), 2.55 (1 H, m, H-3a), 1.93–1.77 (3 H, m, H-2, H-3b), 1.61 (1 H, dd,  $J = 8.1, 3.6$  Hz, H-5), 0.73 (1 H, m, H-6a), 0.61 (1 H, m, H-6b).

(1*S*,5*R*)-4-Dimethoxymethyl-1-hydroxymethylbicyclo[3.1.0]hexane (**11**, diastereomixture). The mixture of **10** (20 mg, 0.13 mmol) and *p*-toluenesulfonic acid monohydrate (5.0 mg, 0.026 mmol) in MeOH (2 mL) was stirred under reflux conditions for 3 h. After the addition of sat. aq.  $\text{NaHCO}_3$  at 0 °C, the resulting mixture was concentrated in reduced pressure. The residue was partitioned between AcOEt and sat. aq.

NaHCO<sub>3</sub>. The organic layer was washed with brine, dried (Na<sub>2</sub>SO<sub>4</sub>), and evaporated. The residue was purified by flash silica gel column chromatography (hexane/AcOEt, 4/1–0/1) to give **11** (20 mg, 0.11 mmol, 85%, diastereomixture, 1/0.8) as a pale yellow liquid.  $[\alpha]_D^{21} = +54.1^\circ$  (c 1.18, CHCl<sub>3</sub>); HRMS (ESI) calcd for C<sub>10</sub>H<sub>18</sub>NaO<sub>3</sub> 209.1148, found 209.1149 [(M + Na)<sup>+</sup>]; Major diastereomer, <sup>1</sup>H-NMR (400 MHz, CDCl<sub>3</sub>) δ 4.10 (1 H, d, J = 9.0 Hz, –CHCH(OMe)<sub>2</sub>), 3.74 (1 H, d, J = 11.4 Hz, –CHaHbOH), 3.43 (1 H, d, J = 11.4 Hz, –CHaHbOH), 3.39 (3 H, s, –OCH<sub>3</sub>), 3.37 (3 H, s, –OCH<sub>3</sub>), 2.24 (1 H, m, H-4), 1.93 (1 H, m, H-3a), 1.82 (1 H, m, H-2a), 1.77 (1 H, m, H-2b), 1.36 (1 H, m, H-3b), 1.18 (1 H, m, H-5), 0.58 (1 H, m, H-6a), 0.45 (1 H, m, H-6b); <sup>13</sup>C NMR (100 MHz, CDCl<sub>3</sub>) δ 107.66, 67.42, 52.99, 52.70, 42.27, 30.72, 28.70, 23.70, 22.74, 8.77; Minor diastereomer, <sup>1</sup>H-NMR (400 MHz, CDCl<sub>3</sub>) δ 4.12 (1 H, d, J = 6.7 Hz, –CHCH(OMe)<sub>2</sub>), 3.64–3.57 (2 H, s, –CH<sub>2</sub>OH), 3.39 (3 H, s, –OCH<sub>3</sub>), 3.31 (3 H, s, CH<sub>3</sub>O–), 2.50 (1 H, m, H-4), 1.82 (1 H, m, H-3a), 1.71–1.62 (2 H, m, H-2a), 1.18 (1 H, m, H-5), 1.02 (1 H, m, H-3b), 0.58 (1 H, m, H-6a), 0.41 (1 H, m, H-6b); <sup>13</sup>C NMR (100 MHz, CDCl<sub>3</sub>) δ 107.15, 67.19, 54.19, 53.15, 42.71, 31.13, 27.19, 23.49, 22.54, 11.85.

(1*S*,4*S*,5*R*)-4-Dimethoxymethyl-1-formylbicyclo[3.1.0]hexane (**12**, *anti*) and (1*S*,4*R*,5*R*)-4-Dimethoxymethyl-1-formylbicyclo[3.1.0]hexane (**13**, *syn*). To a solution of **11** (152 mg, 0.816 mmol) in DMSO (9.0 mL) were added Et<sub>3</sub>N (0.349 mL, 2.46 mmol) and pyridine–SO<sub>3</sub> complex (262 mg, 1.64 mmol), and the mixture was stirred at rt for 3 h. After the addition of sat. aq. NH<sub>4</sub>Cl, the mixture was partitioned between AcOEt and sat. aq. NH<sub>4</sub>Cl. The organic layer was washed with brine, dried (Na<sub>2</sub>SO<sub>4</sub>), and evaporated. The residue was purified by flash silica gel column chromatography (hexane/AcOEt, 8/1) to give **12** (43 mg, 0.23 mmol, 29%, *anti*, less polar) as a colorless oil and **13** (78 mg, 0.43 mmol, 52%, *syn*, more polar) as a colorless oil. **12**:  $[\alpha]_D^{21} = -2.6^\circ$  (c 0.99, CHCl<sub>3</sub>); <sup>1</sup>H-NMR (400 MHz, CDCl<sub>3</sub>) δ 8.90 (1 H, s, CHO), 3.98 (1 H, d, J = 8.2 Hz, –CHCH(OMe)<sub>2</sub>), 3.28 (3 H, s, –OCH<sub>3</sub>), 3.26 (3 H, s, –OCH<sub>3</sub>), 2.26 (1 H, dd, J = 8.2, 7.7 Hz, H-4), 2.16 (1 H, m, H-3a), 1.96 (1 H, dd, J = 9.1, 5.4 Hz, H-5), 1.73 (1 H, dd, J = 14.0, 8.6 Hz, H-2a), 1.64 (1 H, dd, J = 13.1, 8.6 Hz, H-5b), 1.40–1.29 (2 H, m, H-3b, H-6a), 1.02 (1 H, dd, J = 5.4, 5.4 Hz, H-6b); <sup>13</sup>C NMR (100 MHz, CDCl<sub>3</sub>) δ 200.19, 105.39, 53.41, 53.34, 42.03, 41.73, 29.44, 23.06, 22.81, 15.68; HRMS (ESI) calcd for C<sub>10</sub>H<sub>16</sub>NaO<sub>3</sub> 207.0992, found 207.0992 [(M + Na)<sup>+</sup>]; **13**:  $[\alpha]_D^{21} = +71.5^\circ$  (c 0.99, CHCl<sub>3</sub>); <sup>1</sup>H-NMR (400 MHz, CDCl<sub>3</sub>) δ 8.87 (1 H, s, CHO), 4.10 (1 H, d, J = 7.7 Hz, –CHCH(OMe)<sub>2</sub>), 3.32 (3 H, s, –OCH<sub>3</sub>), 3.26 (3 H, s, –OCH<sub>3</sub>), 2.48 (1 H, m, H-4), 2.23 (1 H, m, H-3a), 1.90 (1 H, m, H-5), 1.76–1.66 (2 H, m, H-2), 1.26 (1 H, dd, J = 8.6, 5.9 Hz, H-6a), 1.16 (1 H, dd, J = 5.9, 5.4 Hz, H-6a), 1.05 (1 H, m, H-3b); <sup>13</sup>C NMR (100 MHz, CDCl<sub>3</sub>) δ 200.12, 106.86, 53.32, 52.81, 41.57, 41.26, 28.71, 23.97, 22.99, 13.24; HRMS (ESI) calcd for C<sub>10</sub>H<sub>16</sub>NaO<sub>3</sub> 207.0992, found 207.0993 [(M + Na)<sup>+</sup>].

(1*S*,4*S*,5*R*)-4-Dimethoxymethyl-1-(1-triphenylmethyl-1*H*-imidazol-4-yl)bicyclo[3.1.0]hexane (**14**). To a suspension of **12** (43 mg, 0.23 mmol) and tosylmethylisocyanide (50 mg, 0.26 mmol) in EtOH (2.3 mL) was added NaOEt (ca. 20% solution in EtOH, 23 μL, 0.053 mmol) at 0 °C, and the mixture was stirred at the same temperature for 3 h. To the reaction mixture was added a saturated NH<sub>3</sub> solution in EtOH (6 mL) at 0 °C, and the resulting mixture was heated at 125 °C for 20 h in a sealed tube. After being cooled to rt, the reaction mixture was concentrated in reduced pressure. The residue was dissolved in CH<sub>2</sub>Cl<sub>2</sub> (3.2 mL), and to the solution were added Et<sub>3</sub>N (96 μL, 0.69 mmol) and TrCl (128 mg, 0.46 mmol). The resulting mixture was stirred at rt for 5 h. After the addition of MeOH, the mixture was partitioned between AcOEt and sat. aq. NaHCO<sub>3</sub>. The organic layer was washed with brine, dried (Na<sub>2</sub>SO<sub>4</sub>), and evaporated. The residue was purified by flash silica gel column chromatography (hexane/AcOEt, 10/1–3/1–1/1) to give **14** (75 mg, 0.12 mmol, 69% in 3 steps) as a pale yellow oil. <sup>1</sup>H-NMR (400 MHz, CDCl<sub>3</sub>) δ 7.32–7.31 (10 H, m, aromatic), 7.15–7.13 (6 H, m, aromatic), 6.54 (1 H, s, imidazole-5), 4.15 (1 H, d, J = 8.1 Hz, –CHCH(OMe)<sub>2</sub>), 3.32 (3 H, s, –OCH<sub>3</sub>), 3.30 (3 H, s, –OCH<sub>3</sub>), 2.30 (1 H, dd, J = 8.1, 7.6 Hz, H-4), 2.02 (1 H, m, H-3a), 1.85 (1 H, dd, J = 12.1, 8.3 Hz, H-2a), 1.72 (1 H, dd, J = 13.9, 8.3 Hz, H-2b), 1.63 (1 H, m, H-5), 1.39 (1 H, m, H-3b), 1.15 (1 H, dd, J = 8.1, 4.5 Hz, H-6a), 0.72 (1 H, dd, J = 4.5, 4.5 Hz, H-6b); <sup>13</sup>C NMR (100 MHz, CDCl<sub>3</sub>) δ 144.6, 142.4, 138.2, 130.0, 129.7, 127.9, 116.3, 106.1, 75.0, 53.5, 52.8, 43.7, 29.0, 27.9, 27.0, 22.9, 14.6; HRMS (ESI) calcd for C<sub>31</sub>H<sub>32</sub>N<sub>2</sub>NaO<sub>2</sub> 487.2356, found 487.2368 [(M + Na)<sup>+</sup>].



(1*S*,4*S*,5*R*)-4-[*N*-(4-Chlorobenzyl)aminomethyl]-1-(1*H*-imidazol-4-yl)bicyclo[3.1.0]hexane dihydrochloride (**6•2HCl**). To a suspension of **14** (49 mg, 0.105 mmol) in hexane (0.20 mL) was added formic acid (0.80 mL), and the mixture was stirred at rt for 3 h. After the addition of sat. aq. NaHCO<sub>3</sub> at 0 °C, the mixture was partitioned between AcOEt and sat. aq. NaHCO<sub>3</sub>. The organic layer was washed with brine, dried (Na<sub>2</sub>SO<sub>4</sub>), and evaporated. The residue was dissolved in CH<sub>2</sub>Cl<sub>2</sub> (3.5 mL), and to the solution was added 4-chlorobenzylamine (0.038 mL, 0.32 mmol), molecular sieves 4Å (powder, 40 mg), and sodium NaBH(OAc)<sub>3</sub> (27 mg, 0.13 mmol), and the mixture was stirred at rt for 15 h. After the addition of sat. aq. NaHCO<sub>3</sub>, the mixture was partitioned between AcOEt and sat. aq. NaHCO<sub>3</sub>. The organic layer was washed with brine, dried (Na<sub>2</sub>SO<sub>4</sub>), and evaporated. The residue was passed through silica gel column chromatography (CHCl<sub>3</sub>/MeOH, 1/0–50/1–9/1) to give a corresponding secondary amine. To a solution of the amine in MeOH (1.1 mL) were added Et<sub>3</sub>N (0.088 mL, 0.63 mmol), *N,N*-dimethyl-4-aminopyridine (DMAP, 3 mg, 0.025 mmol), and Boc<sub>2</sub>O (0.113 mL, 0.54 mmol), and the mixture was stirred at rt for 5 h. The reaction mixture was concentrated in reduced pressure, and the residue was purified by flash silica gel column chromatography (hexane/AcOEt, 15/1–2/1) to give a corresponding *N*-Boc-amine (33 mg, 0.051 mmol) as a pale yellow oil. To a solution of *N*-Boc-amine (33 mg) in EtOH (1.1 mL) was added aq. HCl (12 M, 0.4 mL), and the mixture was stirred under reflux conditions for 3 h. After being cooled to rt, the reaction mixture was concentrated in reduced pressure. The residue was partitioned between aq. HCl (2 M) and CH<sub>2</sub>Cl<sub>2</sub>. The aqueous layer was neutralized by aq. NaOH (2 M) and partitioned between aq. NaOH (2 M) and CH<sub>2</sub>Cl<sub>2</sub>. The organic layer was washed with brine, dried (Na<sub>2</sub>SO<sub>4</sub>), and evaporated. The residue was purified by NH silica gel column chromatography (CHCl<sub>3</sub>/MeOH, 1/0–50/1) to give **6** as a free amine. **6** was dissolved in a solution of HCl in MeOH (2 M), and the mixture was concentrated in reduced pressure. The residue was triturated with Et<sub>2</sub>O to give **6•2HCl** (19 mg, 0.051 mmol, 49% in 4 steps) as a hygroscopic white solid.  $[\alpha]_D^{29} = +16.0^\circ$  (*c* 0.66, CH<sub>3</sub>OH); <sup>1</sup>H-NMR (400 MHz, CD<sub>3</sub>OD)  $\delta$  8.81 (1 H, s, imidazole-2), 7.62–7.61 (2 H, d, *J* = 8.0 Hz, aromatic), 7.47–7.43 (3 H, m, aromatic and imidazole-5), 4.28 (2 H, s, benzyl), 3.19 (1 H, m, –CHCHaHbN–), 3.11 (1 H, m, –CHCHaHbN–), 2.54 (1 H, m, H-4), 2.23–2.08 (2 H, m, H-2a, and H-3a), 1.86 (1 H, m, H-5), 1.78 (1 H, m, H-2b), 1.66 (1 H, m, H-3b), 1.13 (2 H, m, H-6); <sup>13</sup>C NMR (100 MHz, CD<sub>3</sub>OD)  $\delta$  138.04, 136.66, 134.60, 133.13, 131.22, 130.25, 116.54, 52.43, 52.11, 39.05, 30.29, 29.85, 25.57, 24.42, 15.19; HRMS (ESI) calcd for C<sub>17</sub>H<sub>21</sub>N<sub>3</sub>Cl 302.1419, found 302.1420 [(M + H)<sup>+</sup>]; Anal. Calcd for C<sub>17</sub>H<sub>20</sub>N<sub>3</sub>Cl•2.1HCl: C, 53.96; H, 5.89; N, 11.11. Found: C, 53.90; H, 5.85; N, 11.07.

#### 4.2. Biological Assay

The protocol of the biological assay was according to the previous report [16]. The membrane preparations of Chinese hamster ovary (CHO) cells, which expressed recombinant human histamine H<sub>3</sub> or H<sub>4</sub> receptors, were purchased from Euroscreen (Brussels, Belgium). The binding assay of the H<sub>3</sub> and H<sub>4</sub> receptors was performed using [<sup>3</sup>H]*N*<sup>α</sup>-methylhistamine (Perkin-Elmer, Boston, MA) and [<sup>3</sup>H]histamine (Perkin-Elmer), respectively. Briefly, the membrane preparations (7.5–15 μg protein) were incubated with different concentrations of [<sup>3</sup>H]*N*<sup>α</sup>-methylhistamine (0.1–3 nM) and of [<sup>3</sup>H]histamine (1–30 nM) for 30 min at 25 °C in 50 mM Tris/5 mM MgCl<sub>2</sub> buffer (pH 7.4). The reaction was terminated by rapid filtration (Cell Harvester, Brandel Co., Gaithersburg, MD) through Whatman GF/B glass fiber filters presoaked for 2 h in 0.5% polyethyleneimine, and the filters were rinsed three times with an ice-cold buffer (2 mL). Membrane-bound radioactivity was extracted from filters overnight in scintillation fluid (toluene, 2 L; Triton X-100, 1 L; 2,5-diphenyloxazole, 15 g; 1,4-bis[2-(5-phenyloxazolyl)]benzene, 0.3 g) and determined in a liquid scintillation counter. The specific binding of each radioligand was determined experimentally from the difference between counts in the presence of 10 μM thioperamide. The apparent dissociation constants (*K*<sub>d</sub>) for each radioligand was determined by nonlinear regression analysis of the curve generated by plotting specific binding concentration versus concentration of the radioligand with GraphPad Prism (GraphPad Software, San Diego, CA) using a one-site binding curve equation. The ability of each compound to inhibit the specific binding of [<sup>3</sup>H]*N*<sup>α</sup>-methylhistamine (1.5 nM) and [<sup>3</sup>H]histamine (25 nM) was estimated by

IC<sub>50</sub> values, which are the molar concentrations of unlabeled drugs necessary for displacing 50% of specific binding (estimated by log probit analysis). The inhibition constant, K<sub>i</sub>, was calculated from the equation,  $K_i = IC_{50}/(1 + L/K_d)$ , where L equals the concentration of each radioligand. The data were presented as mean ± SE (n = 3–5).

## 5. Conclusions

The imidazolyl bicyclo[3.1.0]hexane derivatives as conformationally restricted histamine analogues designed and synthesized in this study showed binding affinity selective for H<sub>3</sub>R over H<sub>4</sub>R, while the parent imidazolylcyclopropane derivatives showed no selectivity. Notably, compound 7 exhibited over 100-fold H<sub>3</sub>R selectivity. The findings of the present study suggest that the imidazolyl bicyclo[3.1.0]hexane structure is a more useful scaffold than the imidazolylcyclopropane structure for the development of selective H<sub>3</sub> receptor ligands. Using both conformationally restricted structures, bicyclo[3.1.0]hexane and cyclopropane with cyclopropylic strain, could allow us to produce more bioactive compounds for structurally unknown proteins, e.g., histamine H<sub>3</sub> and H<sub>4</sub> receptors, effectively.

**Supplementary Materials:** The followings are available online: Figures S1–S3; Schemes S1 and S2; Synthetic procedures and characterization of compounds 7, *ent*-6, and *ent*-7; <sup>1</sup>H-NMR spectra of compounds 6, 7, *ent*-6, and *ent*-7.

**Author Contributions:** M.W., T.K. and S.S. conceived this work, designed the compounds, performed the synthesis, and analyzed the data; Y.I. and S.Y. performed the biological assays and analyzed the data; M.W. and S.S. wrote the paper. All authors have read and agreed to the published version of the manuscript.

**Funding:** This research was funded by MEXT/JSPS KAKENHI Grant Numbers JP19H01014 (to SS), JP19K06965 (to MW), and a research grant from Takeda Science Foundation (to MW), and partly by Platform Project for Supporting Drug Discovery and Life Science Research (BINDS) from AMED under Grant Number JP18am0101093.

**Acknowledgments:** We are grateful to Sanyo Fine Co., Ltd. for the gift of the chiral epichlorohydrin.

**Conflicts of Interest:** The authors declare no conflict of interest.

## References

1. Arrang, J.M.; Garbarg, M.; Schwartz, J.C. Auto-inhibition of brain histamine-release mediated by a novel class (H-3) of histamine-receptor. *Nature* **1983**, *302*, 832–837. [[CrossRef](#)] [[PubMed](#)]
2. Lovenberg, T.W.; Roland, B.L.; Wilson, S.J.; Jiang, X.X.; Pyati, J.; Huvar, A.; Jackson, M.R.; Erlander, M.G. Cloning and functional expression of the human histamine H-3 receptor. *Mol. Pharmacol.* **1999**, *55*, 1101–1107. [[CrossRef](#)] [[PubMed](#)]
3. Leurs, R.; Bakker, R.A.; Timmerman, H.; de Esch, I.J.P. The histamine H<sub>3</sub> receptor: From gene cloning to H<sub>3</sub> receptor drugs. *Nat. Rev. Drug Discov.* **2005**, *4*, 107–120. [[CrossRef](#)] [[PubMed](#)]
4. Celanire, S.; Wijtmans, M.; Talaga, P.; Leurs, R.; de Esch, I.J.P. Histamine H-3 receptor antagonists reach out for the clinic. *Drug Discov. Today* **2005**, *10*, 1613–1627. [[CrossRef](#)]
5. Berlin, M.; Boyce, C.W.; Ruiz Mde, L. Histamine H<sub>3</sub> receptor as a drug discovery target. *J. Med. Chem.* **2011**, *54*, 26–53.
6. Romigi, A.; Vitrani, G.; Lo Giudice, T.; Centonze, D.; Franco, V. Profile of pitolisant in the management of narcolepsy: Design, development, and place in therapy. *Drug Des. Devel. Ther.* **2018**, *12*, 2665–2675. [[CrossRef](#)]
7. Łażewska, D.; Kieć-Kononowicz, K. Progress in the development of histamine H<sub>3</sub> receptor antagonists/inverse agonists: A patent review (2013–2017). *Expert Opin. Ther. Pat.* **2018**, *28*, 175–196. [[CrossRef](#)]
8. Liu, C.L.; Ma, X.J.; Jiang, X.X.; Wilson, S.J.; Hofstra, C.L.; Blevitt, J.; Pyati, J.; Li, X.B.; Chai, W.Y.; Carruthers, N.; et al. Cloning and pharmacological characterization of a fourth histamine receptor (H-4) expressed in bone marrow. *Mol. Pharmacol.* **2001**, *59*, 420–426. [[CrossRef](#)]
9. Nguyen, T.; Shapiro, D.A.; George, S.R.; Setola, V.; Lee, D.K.; Cheng, R.; Rauser, L.; Lee, S.P.; Lynch, K.R.; Roth, B.L.; et al. Discovery of a novel member of the histamine receptor family. *Mol. Pharmacol.* **2001**, *59*, 427–433. [[CrossRef](#)]
10. Mizuno, A.; Matsui, K.; Shuto, S. From peptides to peptidomimetics: A strategy based on the structural features of cyclopropane. *Chem. Eur. J.* **2017**, *23*, 14394–14409. [[CrossRef](#)]

11. Kazuta, Y.; Matsuda, A.; Shuto, S. Development of versatile *cis*- and *trans*-dicarbon-substituted chiral cyclopropane units: Synthesis of (1*S*,2*R*)- and (1*R*,2*R*)-2-aminomethyl-1-(1*H*-imidazol-4-yl)cyclopropanes and their enantiomers as conformationally restricted analogues of histamine. *J. Org. Chem.* **2002**, *67*, 1669–1677. [[CrossRef](#)] [[PubMed](#)]
12. Kazuta, Y.; Hirano, K.; Natsume, K.; Yamada, S.; Kimura, R.; Matsumoto, S.-i.; Furuichi, K.; Matsuda, A.; Shuto, S. Cyclopropane-based conformational restriction of histamine. (1*S*,2*S*)-2-(2-Aminoethyl)-1-(1*H*-imidazol-4-yl)cyclopropane, a highly selective agonist for the histamine H<sub>3</sub> receptor, having a *cis*-cyclopropane structure. *J. Med. Chem.* **2003**, *46*, 1980–1988. [[PubMed](#)]
13. Watanabe, M.; Yamaguchi, K.; Tang, W.; Yoshida, K.; Silverman, R.B.; Arisawa, M.; Shuto, S. Synthesis of a series of 3,4-methanoarginines as side-chain conformationally restricted analogues of arginine. *Bioorg. Med. Chem.* **2011**, *19*, 5984–5988. [[CrossRef](#)] [[PubMed](#)]
14. Watanabe, M.; Kobayashi, T.; Hirokawa, T.; Yoshida, A.; Ito, Y.; Yamada, S.; Orimoto, N.; Yamasaki, Y.; Arisawa, M.; Shuto, S. Cyclopropane-based stereochemical diversity-oriented conformational restriction strategy: Histamine H<sub>3</sub> and/or H<sub>4</sub> receptor ligands with the 2,3-methanobutane backbone. *Org. Biomol. Chem.* **2012**, *10*, 736–745. [[CrossRef](#)] [[PubMed](#)]
15. Nakada, K.; Yoshikawa, M.; Ide, S.; Suemasa, A.; Kawamura, S.; Kobayashi, T.; Masuda, E.; Ito, Y.; Hayakawa, W.; Katayama, T.; et al. Cyclopropane-based conformational restriction of GABA by a stereochemical diversity-oriented strategy: Identification of an efficient lead for potent inhibitors of GABA transports. *Bioorg. Med. Chem.* **2013**, *21*, 4938–4950. [[CrossRef](#)]
16. Watanabe, M.; Kazuta, Y.; Hayashi, H.; Yamada, S.; Matsuda, A.; Shuto, S. Stereochemical diversity-oriented conformational restriction strategy. Development of potent histamine H-3 and/or H-4 receptor antagonists with an imidazolylcyclopropane structure. *J. Med. Chem.* **2006**, *49*, 5587–5596.
17. Kiss, R.; Keseru, G.M. Novel histamine H<sub>4</sub> receptor ligands and their potential therapeutic applications: An update. *Expert Opin. Ther. Pat.* **2014**, *24*, 1185–1197. [[CrossRef](#)]
18. Watanabe, M.; Hirokawa, T.; Kobayashi, T.; Yoshida, A.; Ito, Y.; Yamada, S.; Orimoto, N.; Yamasaki, Y.; Arisawa, M.; Shuto, S. Investigation of the bioactive conformation of histamine H<sub>3</sub> receptor antagonists by the cyclopropyl strain-based conformational restriction strategy. *J. Med. Chem.* **2010**, *53*, 3585–3593.
19. Kobayashi, T.; Suemasa, A.; Igawa, A.; Ide, S.; Fukuda, H.; Abe, H.; Arisawa, M.; Minami, M.; Shuto, S. Conformationally restricted GABA with bicyclo[3.1.0]hexane backbone as the first highly selective BGT-1 inhibitor. *ACS Med. Chem. Lett.* **2014**, *5*, 889–893. [[CrossRef](#)]
20. Horne, D.A.; Yakusijin, K.; Büchi, G. A two-step synthesis of imidazoles from aldehydes via 4-tosylloxazolines. *Heterocycles* **1994**, *39*, 139–153.
21. Shuto, S.; Ono, S.; Imoto, H.; Yoshii, K.; Matsuda, A. Synthesis and biological activity of conformationally restricted analogues of milnacipran: (1*S*,2*R*)-1-phenyl-2-[(*R*)-1-amino-2-propynyl]-*N,N*-diethylcyclopropanecarboxamide is a novel class of NMDA receptor channel blocker. *J. Med. Chem.* **1998**, *41*, 3507–3514. [[PubMed](#)]
22. Kawamura, S.; Unno, Y.; Tanaka, M.; Sasaki, T.; Yamano, A.; Hirokawa, T.; Kameda, T.; Asai, A.; Arisawa, M.; Shuto, S. Investigation of the noncovalent binding mode of covalent proteasome inhibitors around the transition state by combined use of cyclopropyl strain-based conformational restriction and computational modeling. *J. Med. Chem.* **2013**, *56*, 5829–5842. [[PubMed](#)]
23. Mizuno, A.; Miura, S.; Watanabe, M.; Ito, Y.; Yamada, S.; Odagami, T.; Kogami, Y.; Arisawa, M.; Shuto, S. Three-dimensional structural diversity-oriented peptidomimetics based on the cyclopropyl strain. *Org. Lett.* **2013**, *15*, 1686–1689. [[CrossRef](#)]
24. Matsui, K.; Kido, Y.; Watari, R.; Kashima, Y.; Yoshida, Y.; Shuto, S. Highly conformationally restricted cyclopropane tethers with three-dimensional structural diversity drastically enhance the cell permeability of cyclic peptides. *Chem. Eur. J.* **2017**, *23*, 3034–3041. [[CrossRef](#)] [[PubMed](#)]

**Sample Availability:** Samples of the compounds are not available from the authors.



© 2020 by the authors. Licensee MDPI, Basel, Switzerland. This article is an open access article distributed under the terms and conditions of the Creative Commons Attribution (CC BY) license (<http://creativecommons.org/licenses/by/4.0/>).